Volume 0 (1981), Number 0 pp. 1–3 COMPUTER GRAPHICS *forum*

Specular Lobe-Aware Filtering and Upsampling for Interactive Indirect Illumination (Supplemental Material)

Y. Tokuyoshi

Square Enix Co., Ltd., Japan

Appendix A: Gaussian Based Weighting Function

This section proves that the Gaussian based weighting function (given by Eq. (2) in the paper) is the special case of our distribution-aware weighting function. In addition, the roles of two user-specified parameters are explained. When $a_i(\mathbf{x}) \propto g\left(\mathbf{x}-\mathbf{x}_i, \tau_i^2\right)$ for $\mathbf{x} \in \mathbb{R}^m$ and $\Omega = \mathbb{R}^m$, we can use $b\left(\mathbf{x}', \mathbf{x}\right) \propto g\left(\mathbf{x}'-\mathbf{x}, \upsilon^2\right)$ where υ^2 is the user-specified parameter. For this case, the smoothed distribution $c_i(\mathbf{x})$ is also a Gaussian function as follows:

$$c_i(\mathbf{x}) \propto g\left(\mathbf{x}-\mathbf{x}_i, \bar{\tau}_i^2\right),$$

where $\bar{\tau}_i^2 = \tau_i^2 + \upsilon^2$. Thus, the normalized distribution function is given by

$$p_i(\mathbf{x}) = \frac{g\left(\mathbf{x}-\mathbf{x}_i, \bar{\tau}_i^2\right)}{\left(\pi\bar{\tau}_i^2\right)^{\frac{m}{4}}}.$$

Therefore, the similarity is derived as

$$q_{i,j} = \left(\frac{2\bar{\tau}_i\bar{\tau}_j}{\bar{\tau}_i^2+\bar{\tau}_j^2}\right)^{\frac{m}{2}} g\left(\mathbf{x}_i-\mathbf{x}_j, \bar{\tau}_i^2+\bar{\tau}_j^2\right),$$

and thus the weighting function is given by

$$w(i,j) = q_{i,j}^{\beta} = \left(\frac{2\bar{\tau}_i\bar{\tau}_j}{\bar{\tau}_i^2+\bar{\tau}_j^2}\right)^{\frac{\beta m}{2}} g\left(\mathbf{x}_i-\mathbf{x}_j, \frac{\bar{\tau}_i^2+\bar{\tau}_j^2}{\beta}\right).$$

The term $\frac{2\bar{\tau}_i\bar{\tau}_j}{\bar{\tau}_i^2+\bar{\tau}_j^2}$ detects the difference of $\bar{\tau}_i$ and $\bar{\tau}_j$ (i.e. difference of τ_i and τ_j). If $\tau_i = \tau_j$, our weighting function is equivalent to the Gaussian based weighting function as follows:

$$w(i,j) = g\left(\mathbf{x}_i-\mathbf{x}_j, \frac{2}{\beta}\tau_i^2 + \frac{2\upsilon^2}{\beta}\right).$$

This variance parameter is the linear transformation of input-dependent variance τ_i^2 using user-specified parameters υ^2 and β. In order to control the kernel bandwidth using this linear transformation, these two parameters are introduced in this paper.

Appendix B: SG Approximation for Parametric BRDFs

Parametric BRDFs are fitted with a single SG by using Wang's on-the-fly analytical approximation [WRG*09]. A BRDF is separated into two factors: the NDF $D_i(\mathbf{h}_i)$, and the rest of the factors $M_i(\psi_i, \omega)$ as follows:

$$\rho(\mathbf{y}_i, \psi_i, \omega) = M_i(\psi_i, \omega) D_i(\mathbf{h}_i),$$

where $\mathbf{h}_i$ is the half-way vector of ψ_i and ω. Bell-shaped NDFs are approximated with an SG. For example, the Phong distribution is approximated as

$$D_i(\mathbf{h}_i) = \frac{n_i+1}{2\pi}(\mathbf{n}_i\cdot\mathbf{h}_i)^{n_i} \approx \mu_i' G\left(\mathbf{h}_i, \mathbf{n}_i, \lambda_i'\right),$$

where n_i is the Phong exponent, $\lambda_i' = n_i$ and $\mu_i' = \frac{n_i+1}{2\pi}$ for this model. Other bell-shaped parametric NDFs (e.g. Beckmann distribution) are also approximated with an SG analytically. Using *spherical warping*, the specular BRDF is approximated as

$$\rho(\mathbf{y}_i, \psi_i, \omega) = M_i(\psi_i, \omega)\mu_i' G(\omega, \xi_i, \lambda_i),$$

where $\xi_i = 2(\mathbf{n}_i\cdot\psi_i)\mathbf{n}_i - \psi_i$, and $\lambda_i = \frac{\lambda_i'}{4(\mathbf{n}_i\cdot\psi_i)}$. Finally, we obtain the following SG approximation:

$$\rho_i(\omega)\max(\mathbf{n}_i\cdot\omega, 0) \approx \mu_i G(\omega, \xi_i, \lambda_i),$$

where $\mu_i = \frac{M_i(\psi_i,\xi_i)\mu_i'\max(\mathbf{n}_i\cdot\xi_i, 0)}{R_i}$. To compute this approximation, the view direction ψ_i, surface normal $\mathbf{n}_i$, reflectance R_i, and BRDF parameters (e.g. n_i) are necessary. For deferred shading pipelines, $\mathbf{n}_i$, R_i and BRDF parameters are given by the G-buffer. The view direction ψ_i is computed with the camera position and the position $\mathbf{y}_i$ which can be given by the position buffer in the G-buffer. Instead of the position buffer, $\mathbf{y}_i$ can be calculated using the camera projection matrix and the depth buffer for memory reduction. Therefore, the parametric specular lobe at each pixel is inexpensively approximated with an SG on-the-fly for real-time

applications with dynamic scenes. ASGs are also usable in the same manner [XSD*13].

Appendix C: Product Integrals of SGs

Spherical Gaussians. The product integral of two SGs is derived in [TS06] as

$$\int_{S^2} G(\omega,\xi_1,\lambda_1)G(\omega,\xi_2,\lambda_2)d\omega = \frac{4\pi\sinh(r)}{\exp(\lambda_1+\lambda_2)r},$$

where $r = \|\lambda_1\xi_1+\lambda_2\xi_2\|$. Since this is not closed in SG basis, Iwasaki et al. [IDN12] introduced the following approximation:

$$\int_{S^2} G(\omega,\xi_1,\lambda_1)G(\omega,\xi_2,\lambda_2)d\omega \approx \frac{2\pi G\left(\xi_1,\xi_2,\frac{\lambda_1\lambda_2}{\lambda_1+\lambda_2}\right)}{\lambda_1+\lambda_2}. \tag{C.1}$$

This approximation error is small if λ_1 or λ_2 are large.

Anisotropic spherical Gaussians. The approximate product integral of an ASG and SG is closed in ASG basis as follows:

$$\begin{aligned}&\int_{S^2} \acute{G}(\omega,\xi_x,\xi_y,\xi_z,\lambda_x,\lambda_y)G(\omega,\xi,\lambda)d\omega\\ \approx\ &\frac{2\pi\acute{G}\left(\xi,\xi_x,\xi_y,\xi_z,\frac{\lambda_x\lambda}{2\lambda_x+\lambda},\frac{\lambda_y\lambda}{2\lambda_y+\lambda}\right)}{\sqrt{(2\lambda_x+\lambda)(2\lambda_x+\lambda)}}.\end{aligned}$$

The approximate integral of an ASG is given by

$$\begin{aligned}&\int_{S^2} \acute{G}\left(\omega,\xi_x,\xi_y,\xi_z,\lambda_x,\lambda_y\right)d\omega\\ \approx\ &\frac{\pi}{\sqrt{\lambda_x\lambda_y}} - \frac{\exp(-\lambda_y)}{2\lambda_x}\left(F(t)-\frac{t}{\lambda_y}F\left(t+\frac{t}{\lambda_y}\right)\right)\\ =\ &B(\lambda_x,\lambda_y),\end{aligned}$$

where $\lambda_x \geq \lambda_y$, $t = \lambda_x - \lambda_y$, and $F(t) = \int_0^{2\pi}\exp\left(-t\cos^2\phi\right)d\phi$ which is approximately obtained with a precomputed 1D texture or an analytical rational approximation. This paper employs the analytical approximation. ASG definition can be equivalently written in algebraic form:

$$\acute{G}(\omega,\mathbf{A}) = \max\left(\omega\cdot\xi_z,0\right)\exp\left(-\omega^T\mathbf{A}\omega\right),$$

where $\mathbf{A}$ is a 3×3 symmetric matrix, and ξ_z is its eigenvector with the smallest eigenvalue. If ASG lobes are not low frequency, the product of two ASGs is approximated with an ASG as the following equation:

$$\acute{G}(\omega,\mathbf{A}_1)\acute{G}(\omega,\mathbf{A}_2) \approx C(\xi_{z,3},\xi_{z,1},\xi_{z,2})\acute{G}(\omega,\mathbf{A}_3),$$

where $\mathbf{A}_3 = \mathbf{A}_1+\mathbf{A}_2$, $\xi_{z,3}$ is the eigenvector with the smallest eigenvalue of $\mathbf{A}_3$, and $C(\xi_{z,3},\xi_{z,1},\xi_{z,2}) = \max(\xi_{z,3}\cdot\xi_{z,1},0)\max(\xi_{z,3}\cdot\xi_{z,2},0)$. Thus, the product integral of two ASGs is approximately obtained as follows:

$$\begin{aligned}&\int_{S^2} \acute{G}(\omega,\mathbf{A}_1)\acute{G}(\omega,\mathbf{A}_2)d\omega\\ \approx\ &C\left(\xi_{z,3},\xi_{z,1},\xi_{z,2}\right)\exp\left(-\lambda'_z\right)B\left(\lambda'_x-\lambda'_z,\lambda'_y-\lambda'_z\right),\end{aligned}$$

where $\lambda'_x,\lambda'_y,\lambda'_z$ are eigenvalues of $\mathbf{A}_3$, and $\lambda'_x \geq \lambda'_y \geq \lambda'_z$.

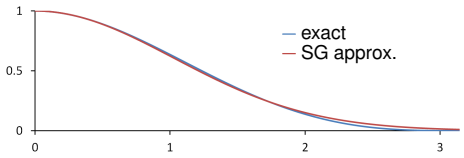

Figure D.1: *Diffuse lobe similarity for* $\kappa = \infty$.

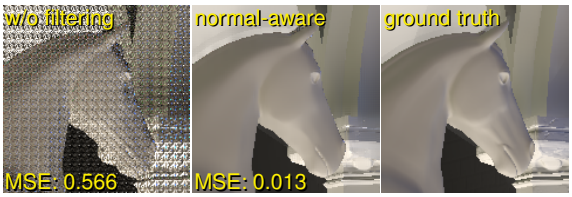

Figure D.2: *Filtering diffuse indirect illumination. Our diffuse lobe-aware filtering is equivalent to the normal-aware filtering. The variance parameter is given as* $\sigma_n^2 = 0.05404477$ *when* $\beta = 20$ *and* $\kappa = 100$.

Appendix D: Diffuse Lobe Similarity

This section reformulates the normal-aware weighting function based on the diffuse lobe similarity. For Lambertian surfaces, the diffuse lobe is given as $a_i(\omega) \propto \max(\mathbf{n}_i\cdot\omega,0)$. As described in Eq. (9) in the paper, the smoothing kernel is an SG with lobe sharpness κ. If $\kappa = \infty$, $c_i(\omega) = a_i(\omega)$ is obtained. Thus the similarity of two diffuse lobes is given by

$$\begin{aligned}q_{i,j} &= \frac{3}{2\pi}\int_{S^2}\max(\mathbf{n}_i\cdot\omega,0)\max(\mathbf{n}_j\cdot\omega,0)d\omega\\ &= \frac{\sin\phi_{i,j}+(\pi-\phi_{i,j})\cos\phi_{i,j}}{\pi},\end{aligned}$$

where $\phi_{i,j} = \arccos(\mathbf{n}_i\cdot\mathbf{n}_j)$. As shown in Fig. D.1, this diffuse lobe similarity is bell-shaped and analogous to an SG as: $q_{i,j} \approx G\left(\mathbf{n}_i,\mathbf{n}_j,\lambda_c\right)$, where the lobe sharpness $\lambda_c = 0.9426$ is obtained by using the least squares method (the integrated squared fitting error: 0.00245). Using Eq. (C.1), this paper extends the above similarity for arbitrary κ as follows:

$$q_{i,j} \approx G\left(\mathbf{n}_i,\mathbf{n}_j,\frac{\lambda_c\kappa}{2\lambda_c+\kappa}\right).$$

Therefore, an SG can be used for the weighting function as

$$w_\omega(i,j) = q_{i,j}^\beta \approx G\left(\mathbf{n}_i,\mathbf{n}_j,\frac{1}{\sigma_n^2}\right) = w_n(i,j).$$

where $\sigma_n^2 = \frac{2\lambda_c+\kappa}{\beta\lambda_c\kappa}$. Hence, the normal-aware weighting function is the special case of our lobe-aware weighting function for diffuse surfaces. This reformulation provides unified parameters κ and β between diffuse and specular surfaces, and reduces material-dependent parameter tuning. Fig. D.2 shows the spatio-temporal filtering using $\beta = 20$ and $\kappa = 100$ for diffuse surfaces.

Appendix E: Code Optimization

Our approximated lobe-aware weighting function (i.e. Eq. (12) in the paper) can be rewritten as follows:

$$\begin{aligned} w_\omega(i,j) &\approx \left(\frac{2\sqrt{\bar{\lambda}_i\bar{\lambda}_j}}{\bar{\lambda}_i+\bar{\lambda}_j}\right)^\beta G\left(\xi_i,\xi_j,\frac{\beta\bar{\lambda}_i\bar{\lambda}_j}{\bar{\lambda}_i+\bar{\lambda}_j}\right) \\ &= \exp\left(\frac{\beta}{2}\log\frac{4u}{v^2}+\frac{\beta u}{v}((\xi_i\cdot\xi_j)-1)\right), \end{aligned}$$

where $u = \bar{\lambda}_i\bar{\lambda}_j$ and $v = \bar{\lambda}_i+\bar{\lambda}_j$. This is used in our implementation for code optimization, because it has only an additional mathematical function (i.e. log) compared to the conventional normal-aware weighting function. In addition, exp and log functions can be compiled using faster intrinsics.

References

[IDN12] IWASAKI K., DOBASHI Y., NISHITA T.: Interactive bi-scale editing of highly glossy materials. *ACM Trans. Graph. 31*, 6 (2012), 144:1–144:7. 2

[TS06] TSAI Y.-T., SHIH Z.-C.: All-frequency precomputed radiance transfer using spherical radial basis functions and clustered tensor approximation. *ACM Trans. Graph. 25*, 3 (2006), 967–976. 2

[WRG*09] WANG J., REN P., GONG M., SNYDER J., GUO B.: All-frequency rendering of dynamic, spatially-varying reflectance. *ACM Trans. Graph. 28*, 5 (2009), 133:1–133:10. 1

[XSD*13] XU K., SUN W.-L., DONG Z., ZHAO D.-Y., WU R.-D., HU S.-M.: Anisotropic spherical gaussians. *ACM Trans. Graph. 32*, 6 (2013), 209:1–209:11. 2